

Azimuthally polarized surface plasmons as effective terahertz waveguides

Qing Cao and Jürgen Jahns

Optische Nachrichtentechnik, FernUniversität Hagen, Universitätsstrasse 27/PRG, D-58084 Hagen, Germany
qing.cao@fernuni-hagen.de

Abstract: Quite recently, it was found that metal wires can effectively guide terahertz radiation. Based on the fact that the absolute values of the relative permittivities of metals in the spectral region of terahertz radiation are huge, we here analyse the properties of this kind of waveguide and explain the related experimental results. In particular, we show that the observed waveguiding is due to the propagation of an azimuthally polarized surface plasmon along the wire. Some related aspects, such as the choice of metal and the slowly decaying modal field, are also discussed. In particular, we show that, if a copper wire with a radius of 0.45 mm is used, the attenuation coefficient is smaller than $2 \times 10^{-3} \text{ cm}^{-1}$ in the whole range of 0.1–1 THz.

© 2005 Optical Society of America

OCIS codes: (260.3090) Infrared, far; (240.6680) Surface plasmon, (230.7370) Waveguides; (260.3910) Metal, optics of.

References and links

1. D. M. Mittleman, ed. *Sensing with Terahertz Radiation* (Springer, Heidelberg, 2002).
2. P. R. Smith, D. H. Auston, and M. C. Nuss, "Subpicosecond photoconducting dipole antennas," *IEEE J. Quant. Electron.* **24**, 255-260 (1998).
3. M. Exter and D. Grischkowsky, "Characterization of an optoelectronic terahertz beam system," *IEEE Trans. Microwave Theory Tech.* **38**, 1684-1691 (1990).
4. P. U. Jepsen, R. H. Jacobsen, and S. R. Keiding, "Generation and detection of terahertz pulses from biased semiconductor antennas," *J. Opt. Soc. Am. B* **13**, 2424-2436 (1996).
5. D. M. Mittleman, R. H. Jacobsen, and M. C. Nuss, "T-ray imaging," *IEEE J. Select. Top. Quant. Electron.* **2**, 679-692 (1996).
6. R. H. Jacobsen, D. M. Mittleman, and M. C. Nuss, "Chemical recognition of gases and gas mixtures with terahertz waves," *Opt. Lett.* **21**, 2011-2013 (1996).
7. R. M. Woodward, V. P. Wallace, D. D. Arnone, E. H. Linfield, and M. Pepper, "Terahertz pulsed imaging of skin cancer in the time and frequency domain," *J. Biol. Phys.* **29**, 257-261 (2003).
8. K. Kawase, Y. Ogawa, and Y. Watanabe, "Non-destructive terahertz imaging of illicit drugs using spectral fingerprints," *Opt. Express* **11**, 2549-2554 (2003).
9. S. Wang and X.-C. Zhang, "Pulsed terahertz tomography," *J. Phys. D* **37**, R1-R36 (2004).
10. R. W. McGowan, G. Gallot, and D. Grischkowsky, "Propagation of ultrawideband short pulses of THz radiation through submillimeter-diameter circular waveguides," *Opt. Lett.* **24**, 1431-1433 (1999).
11. G. Gallot, S. P. Jamison, R. W. McGowan, and D. Grischkowsky, "Terahertz waveguides," *J. Opt. Soc. Am. B* **17**, 851-863 (2000).
12. R. Mendis and D. Grischkowsky, "Plastic ribbon THz waveguides," *J. Appl. Phys.* **88**, 4449-4451 (2000).
13. S. P. Jamison, R. W. McGowan, and D. Grischkowsky, "Single-mode waveguide propagation and reshaping of sub-ps terahertz pulses in sapphire fiber," *Appl. Phys. Lett.* **76**, 1987-1989 (2000).
14. R. Mendis and D. Grischkowsky, "Undistorted guided-wave propagation of subpicosecond terahertz pulses," *Opt. Lett.* **26**, 846-848 (2001).
15. R. Mendis and D. Grischkowsky, "THz interconnect with low loss and low group velocity dispersion," *IEEE Microwave Wireless Comp. Lett.* **11**, 444-446 (2001).
16. S. Coleman and D. Grischkowsky, "A THz transverse electromagnetic mode two-dimensional interconnect layer incorporating quasi-optics," *Appl. Phys. Lett.* **83**, 3656-3658 (2003).
17. K. Wang and D. M. Mittleman, "Metal wires for terahertz wave guiding," *Nature (London)*, **432**, 376-379 (2004).
18. H. Raether, *Surface Plasmons on Smooth and Rough Surfaces and on Gratings*, (Springer, Berlin, 1988).
19. <http://www.surfaceplasmonoptics.org>

20. Q. Cao and Ph. Lalanne, "Negative role of surface plasmons in the transmission of metallic gratings with very narrow slits," *Phys. Rev. Lett.* **88**, 057403 (2002).
21. S. I. Bozhevolnyi, "Waveguiding in surface plasmon polariton band gap structures," *Phys. Rev. Lett.* **86**, 3008-3011 (2001).
22. M. I. Stockman, "Nanofocusing of optical energy in tapered plasmonic waveguides," *Phys. Rev. Lett.* **93**, 137404 (2004).
23. C. A. Pfeiffer, E. N. Economou, and K. L. Ngai, "Surface polaritons in a circularly cylindrical interface: surface plasmons," *Phys. Rev. B* **10**, 3038-3051 (1974).
24. U. Schröter and A. Dereux, "Surface plasmon polaritons on metal cylinders with dielectric core," *Phys. Rev. B* **64**, 125420 (2001).
25. M. Born and E. Wolf, *Principles of Optics*, 5th ed. (Pergamon Press, Oxford, 1975).
26. G. N. Watson, *A Treatise on the Theory of Bessel Functions*, 2nd ed. (Cambridge U. Press, Cambridge, UK 1966).
27. M. A. Ordal, R. J. Bell, R. W. Alexander, L. L. Long, and M. R. Querry, "Optical properties of fourteen metals in the infrared and far infrared: Al, Co, Cu, Au, Fe, Pb, Mo, Ni, Pd, Pt, Ag, Ti, V, and W," *Appl. Opt.* **24**, 4493-4499 (1985).
28. <http://hyperphysics.phy-astr.gsu.edu/hbase/tables/magprop.html#c1>
29. <http://www.stainless-rebar.org/grades.htm>
30. C. Weber and J. Fajans, "Saturation in "nonmagnetic" stainless steel," *Rev. Scientific Instruments* **69**, 3695-3696 (1998).
31. S. Quabis, R. Dorn, M. Eberler, O. Glöckl, and G. Leuchs, "Focusing light to a tighter spot," *Opt. Commun.* **179**, 1-7 (2000).
32. R. Dorn, S. Quabis, and G. Leuchs, "Sharper focus for a radially polarized light beam," *Phys. Rev. Lett.* **91**, 233901 (2003).
33. Q. Zhan and J. R. Leger, "Focus shaping using cylindrical vector beams," *Opt. Express* **10**, 324-331 (2002).

1. Introduction

The terahertz (THz) region of the electromagnetic spectrum is located between microwave and optical frequencies, normally defined as the range from 0.1 to 10 THz (or correspondingly, from 30 μm to 3 mm in wavelength). In recent years, THz radiation has attracted a lot of interests [1-9], because it offers significant scientific and technological potential in many fields, such as in sensing, in imaging, and in spectroscopy. However, waveguiding in this intermediate spectral region is still a challenge [10-16]. Both of the conventional metal waveguides for microwave radiation and the dielectric fibers for visible radiation cannot be used to effectively guide THz radiation. The obstacles come from the high loss from the finite conductivity of metals or the high absorption coefficient of dielectric materials in this spectral range. Quite recently, Wang and Mittleman [17] found that a simple metal wire can be used as effective THz waveguide. This finding paves the way for a wide range of new applications for THz sensing and imaging. In Ref. [17], the authors focused on the report of experimental observations, however, without a deep theoretical explanation.

In this paper, we present the needed theory and explain the related experimental results. In particular, we show that the observed waveguiding effect is due to the propagation of an azimuthally polarized surface plasmon (APSP) along the wire. In addition, we also discuss some related problems. In particular, we suggest the use of copper wires instead of stainless steel wires as more effective THz waveguides.

2. Explanations for THz metal wire waveguides

It is well known that there exists an electromagnetic bound state at a flat metal-dielectric interface. This bound state can only exist for the TM polarization and is called surface plasmon (SP) [18, 19]. SPs can be excited by periodic structures like metal gratings [20], and can propagate along flat metal-dielectric interfaces [21]. Similar to THz radiation, SPs have also attracted much attention in recent years [19].

It is relatively less well known that SP can also exist at a cylindrical metal-dielectric interface [22-24]. For an SP at a flat metal-dielectric interface, there are one magnetic field component H_y , and two electrical field components E_x and E_z . The only transverse magnetic field component H_y indicates the TM polarization. For an SP at a cylindrical metal-dielectric interface, however, there are one magnetic field component H_ϕ , and two electric field

components E_r and E_z . The only transverse magnetic field component H_ϕ indicates the TM polarization. The latter kind of SP can be reasonably called APSP, because the only magnetic field component H_ϕ is angular.

Consider the eigenproblem of a cylindrical metal wire surrounded by air. We denote by ϵ and μ the relative permittivity and the relative magnetic permeability, respectively. For the metal, we use ϵ_m and μ_m . And for air, $\epsilon=\mu=1$. We denote by λ_0 , c , and R the wavelength in free space, the light speed in free space, and the radius of the metal wire, respectively. We assume a temporal factor $\exp(-j\omega t)$, where $\omega=2\pi c/\lambda_0$, is the angular frequency.

We are interested in axially symmetrical eigenmodes. For them, the relations $\partial\mathbf{E}/\partial\phi=0$ and $\partial\mathbf{H}/\partial\phi=0$ hold in the cylindrical coordinates. By use of these relations, one can separate the electromagnetic field into two families. One is the TE polarization, and the other is the TM polarization. For the former, there are three components E_ϕ , H_r and H_z . For the latter, there are another three components H_ϕ , E_r and E_z . The two families of TE and TM polarizations are decoupling in this case. We now focus on the TM polarization. By substituting the relations $\partial\mathbf{E}/\partial\phi=0$ and $\partial\mathbf{H}/\partial\phi=0$ into Maxwell's equations [25], one obtains

$$H_\phi = \frac{-j}{\mu k_0} \left(\frac{\partial E_r}{\partial z} - \frac{\partial E_z}{\partial r} \right), \quad (1)$$

$$E_z = \frac{j}{\epsilon k_0} \frac{1}{r} \frac{\partial}{\partial r} (r H_\phi), \quad (2)$$

$$E_r = \frac{-j}{\epsilon k_0} \frac{\partial H_\phi}{\partial z}. \quad (3)$$

All of H_ϕ , E_r and E_z are functions of the two variables r and z . For the formulation of the eigenproblem, they can be written as $H_\phi(r,z) = H_\phi(r)\exp(jk_0 n_{\text{eff}} z)$, $E_r(r,z) = E_r(r)\exp(jk_0 n_{\text{eff}} z)$, and $E_z(r,z) = E_z(r)\exp(jk_0 n_{\text{eff}} z)$, respectively, where n_{eff} is the effective index of the eigenmode. Then the operator $\partial/\partial z$ can be replaced by $jk_0 n_{\text{eff}}$. In the remainder of this paper, we refer to H_ϕ , E_r and E_z specifically as $H_\phi(r)$, $E_r(r)$ and $E_z(r)$, respectively. By using the relation $\partial/\partial z = jk_0 n_{\text{eff}}$ in Eq. (3), one gets

$$E_r = \epsilon^{-1} n_{\text{eff}} H_\phi. \quad (4)$$

Substituting Eq. (4) into Eq. (1), and using the relation $\partial/\partial z = jk_0 n_{\text{eff}}$ again, one can obtain

$$H_\phi = \frac{j\epsilon}{k_0(\mu\epsilon - n_{\text{eff}}^2)} \frac{dE_z}{dr}, \quad (5)$$

Further substituting Eq. (5) into Eq. (2), one can obtain

$$\rho^2 \frac{d^2 E_z}{d\rho^2} + \rho \frac{dE_z}{d\rho} - \rho^2 E_z = 0, \quad (6)$$

where $\rho = k_0[(n_{\text{eff}})^2 - \mu\epsilon]^{1/2} r$. The suitable solution for E_z has the form $I_0(k_0 \kappa_m r)$ in the metal and $K_0(k_0 \kappa_a r)$ in air, because this solution approximately decays exponentially from the interface, where $I_0(\cdot)$ and $K_0(\cdot)$ are the generalized Bessel functions [26], $\kappa_m = [(n_{\text{eff}})^2 - \mu_m \epsilon_m]^{1/2}$ and $\kappa_a = [(n_{\text{eff}})^2 - 1]^{1/2}$. Substituting this kind of solution into Eq. (5), and using the relations [26] $dI_0(k_0 \kappa_m r)/dr = k_0 \kappa_m I_1(k_0 \kappa_m r)$ and $dK_0(k_0 \kappa_a r)/dr = -k_0 \kappa_a K_1(k_0 \kappa_a r)$, one can determine the solution form of H_ϕ . By using the continuities of E_z and H_ϕ at the interface $r=R$, one can obtain the following eigenvalue equation

$$\frac{\epsilon_m}{\kappa_m} \frac{I_1(k_0 \kappa_m R)}{I_0(k_0 \kappa_m R)} + \frac{1}{\kappa_a} \frac{K_1(k_0 \kappa_a R)}{K_0(k_0 \kappa_a R)} = 0. \quad (7)$$

The existence of the solution of Eq. (7) results from the negative real part of ϵ_m . This negative value is due to the electron plasma contribution when the frequency is lower than the plasma frequency. Accordingly, this eigenmode is traditionally called SP. In particular, when $R \rightarrow \infty$,

the relations $I_1(k_0\kappa_m R)/I_0(k_0\kappa_m R)=1$ and $K_1(k_0\kappa_a R)/K_0(k_0\kappa_a R)=1$ hold. By use of these properties, one can obtain, for very large R ,

$$n_{\text{eff}} = \sqrt{\frac{\epsilon_m(\epsilon_m - \mu_m)}{(1 + \epsilon_m)(\epsilon_m - 1)}}. \quad (8)$$

Eq. (8) is exactly valid for an SP at a flat metal-air interface. It can be expected that Eq. (8) is also approximately valid for an APSP at the interface of a very thick metal wire. In particular, for nonmagnetic metals with $\mu_m=1$, Eq. (8) reduces to $n_{\text{eff}}=[\epsilon_m/(1+\epsilon_m)]^{1/2}$. Eq. (8) is already enough for some qualitative analyses, though the exact n_{eff} value of the APSP should be obtained by numerically solving Eq. (7).

We now briefly discuss the dimensions of the APSP modal field. For simplicity, we discuss the only magnetic field component $H_\phi(r)$. The $H_\phi(r)$ field is proportional to $K_1(k_0\kappa_a r)/K_0(k_0\kappa_a R)$ outside the metal. As we shall point out below, n_{eff} is approximately equal to 1. As a consequence, κ_a is very small. Because κ_a is very small, then the field distribution $K_1(k_0\kappa_a r)/K_0(k_0\kappa_a R)$ decays very slowly with the radial coordinate r . Typically, the modal field has a width of about several tens times of the radius R outside the metal. In the metal, the $H_\phi(r)$ field is proportional to $I_1(k_0\kappa_m r)/I_0(k_0\kappa_m R)$. As we shall see below, $|\epsilon_m|$ is far larger than 1 in the THz spectral region. Using the relations $|\epsilon_m| \gg 1$ and $n_{\text{eff}} \approx 1$, one can get the relation $\kappa_m \approx (-\epsilon_m)^{1/2}$. As a consequence, the real part of κ_m is quite large. Typically, it has the order of magnitude of 1.0×10^3 or larger. This property leads to the fast decay of the modal field in the metal. Typically, the modal field can exist in the metal for only about $1 \mu\text{m}$ or less. Therefore, the modal field of an APSP has a very large beam width but with a hollow center.

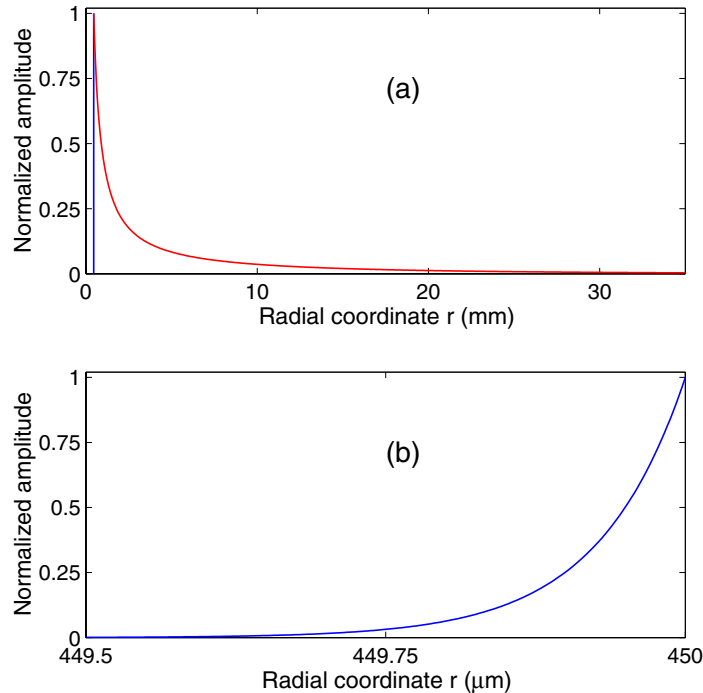


Fig. 1. Normalized modal field of an APSP of a copper wire. The red curve is the modal field outside the metal, and the blue curves are the modal field in the metal. (a) The total profile. (b) The detailed distribution of the very small penetration of the modal field in the metal.

To get an intuitive impression, we calculate the $H_\phi(r)$ field distribution of an APSP of a copper wire with a radius of 0.45 mm . The frequency is 0.5 THz (the corresponding wavelength is 0.6 mm). The related calculation method used here will be stated in Section 3.

From Fig. 1(a), one can see that the modal field outside the metal has a long tail of about 20 mm. In contrast, the modal field decays very fast in the metal. From Fig. 1(b), one can see that the penetration depth in the metal is smaller than 0.5 μm .

We now attribute the observed waveguiding of a metal wire [17] to the propagation of an APSP along the wire. In the following, we try to use this model to explain the related experimental results of Ref. [17].

1). It is well known that the absolute values of ϵ_m of metals are huge in the spectral region of THz radiation. This property can be deduced from the Drude model [25, 27]. Typically [27], $-\text{Re}(\epsilon_m)$ is larger than 10^4 and $\text{Im}(\epsilon_m)$ is larger than 10^5 , where $\text{Re}(\cdot)$ and $\text{Im}(\cdot)$ indicate the real and the imaginary parts, respectively. By using the properties $|\epsilon_m| \gg 1$ and $|\epsilon_m| \gg \mu_m$ in Eq. (8), one can find that $n_{\text{eff}} \approx 1$. This result explains the low loss of metal wire waveguides because $\text{Im}(n_{\text{eff}})$ is very small.

2). The relation $n_{\text{eff}} \approx 1$ holds for a very wide bandwidth, because $|\epsilon_m|$ is huge in the whole range of THz radiation. This property explains the very low dispersion of metal wire waveguides.

3). It can be proved that the ration $|E_z/E_r|$ is in the order of magnitude of $|\kappa_a/n_{\text{eff}}|$ in air. By using the relation $n_{\text{eff}} \approx 1$, one can find that $|E_z| \ll |E_r|$. This property implies that the longitudinal field component E_z is negligible in air. As a result, the modal field is an approximate TEM field in air. Note that it is no longer true in the metal. In the metal, $|E_r| \ll |E_z|$. It is worth mentioning that, it is not the radial field component E_r but the longitudinal field component E_z that leads to the attenuation of the eigenmode.

4). Because the longitudinal field E_z is negligible, the remaining only electric field component in air is E_r . Then it looks like that the electric field is radially polarized.

5). The electrical field of the light source is linearly polarized, but the electric field of the APSP is approximately radially polarized. The polarization mismatch between them leads to a very low coupling efficiency, though some additional setup was used to help the coupling.

6). As we state above, the modal field is quite large. As a result, the guided propagation can be easily coupled between two waveguides that are in contact with each other.

7). As stated above, the modal field is slowly decaying outside the metal. As a result, almost all of the energy is propagated in air whose refractive index is 1. Also, $n_{\text{eff}} \approx 1$. These two properties imply that the Fresnel reflectivity at the end of metal wire is negligible. Therefore, the mode can propagate off the end of the waveguide.

8). The metal wire is axially symmetric. For axially symmetric electromagnetic fields, TM and TE polarizations are decoupling. Thus, the radial polarization of the electric field can be maintained during propagation, even after propagating off the end of the metal wire.

9). The beam width of the modal field is quite large because it decays slowly outside the metal. As a result, the waveguide can be only slightly curved. Otherwise, emission due to waveguide bending may happen.

Clearly, these excellent explanations confirm that the waveguide effect of a metal wire is indeed due to the propagation of an APSP. It is worth mentioning that, besides the zero-order SP (i.e., APSP) mentioned above, there also exist higher-order SPs [23]. However, they are not really guided modes. In fact, those higher-order modes were called virtual radiative SPs in Ref. [23], in contrast to APSP, which is called real nonradiative SP in Ref. [23]. Therefore, the existence of those virtual radiative SPs does not affect our analyses.

3. Further discussions

In Section 2 we have explained the experimental results of Ref. [17]. In this Section we discuss some further problems.

As we state above, the low loss and the very low dispersion of an APSP come from the huge absolute values $|\epsilon_m|$. In the spectral region of THz radiation, different metals still have different $|\epsilon_m|$ [27] though those values are all huge. For example, the value $|\epsilon_m|$ of copper is more than 10 times higher than that of iron [27]. Generally speaking, the larger the value $|\epsilon_m|$, the better the waveguide. In addition, the relative magnetic permeability μ_m also plays a role.

By use of a Taylor expansion of Eq. (8) for huge ϵ_m , one can prove that $n_{\text{eff}} \approx 1 - \mu_m / (2\epsilon_m)$. From this expression, one can deduce that, for the same ϵ_m , a magnetic metal will increase the loss by μ_m times. Therefore, the use of ferromagnetic metal [25, 28], such as iron and nickel, should be avoided. We suggest the use of nonmagnetic metals with very large $|\epsilon_m|$. Copper, silver and gold are good candidates. Copper, of course, would be preferable because it is much cheaper than silver and gold. We notice that stainless steel wires are used in the experiments of Ref. [17]. Stainless steels can be magnetic or “nonmagnetic” [29, 30], depending on the kinds. In Ref. [17], there is no report about the μ_m value of the used stainless steel. Therefore, it is difficult to concretely calculate the waveguide parameters of the stainless steel wires used there [17]. However, the μ_m value should be not smaller than 1 [30]. Also, the $|\epsilon_m|$ value of a stainless steel should be smaller than that of copper, because the $|\epsilon_m|$ value of iron, which is the main chemical composition of stainless steel, is at least 10 times smaller than that of copper [27]. Therefore, a copper wire waveguide is superior to a stainless steel wire waveguide.

As we state above, the exact n_{eff} value can only be obtained by numerically solving the eigenvalue equation (7), though Eq. (8) is very useful for qualitative analyses. It is known that both the functions $I_1(\cdot)$ and $I_0(\cdot)$ approximately increase exponentially with the increase of the real part of the argument. Unfortunately, the real part of the argument $k_0\kappa_m R$ is quite large in the investigated case. For example, in the example of Fig. 1, the argument $k_0\kappa_m R$ is as large as $6.21 \times 10^3 - j4.95 \times 10^3$. Because the argument $k_0\kappa_m R$ is quite large, numerical overflow will happen if one directly calculates the functions $I_1(k_0\kappa_m R)$ and $I_0(k_0\kappa_m R)$ that appear in Eq. (7). To solve this problem, we use the asymptotic expression [26]

$$I_\nu(u) \approx \frac{\exp(u)}{(2\pi u)^{1/2}} \left[1 - \frac{4\nu^2 - 1}{8u} + \frac{(4\nu^2 - 1)(4\nu^2 - 9)}{2(8u)^2} \right]$$

where ν is the order and u is the argument. By using this relation in the ratio $I_1(k_0\kappa_m R)/I_0(k_0\kappa_m R)$, the diverging factor $\exp(k_0\kappa_m R)$ is removed and the overflow is overcome. Then the eigenvalue equation (7) can be solved by complex-root search methods. Local search methods would be effective. We use the Newton method to solve the eigenvalue problem. Once obtaining the eigenvalue n_{eff} , one can immediately obtain the complete modal field.

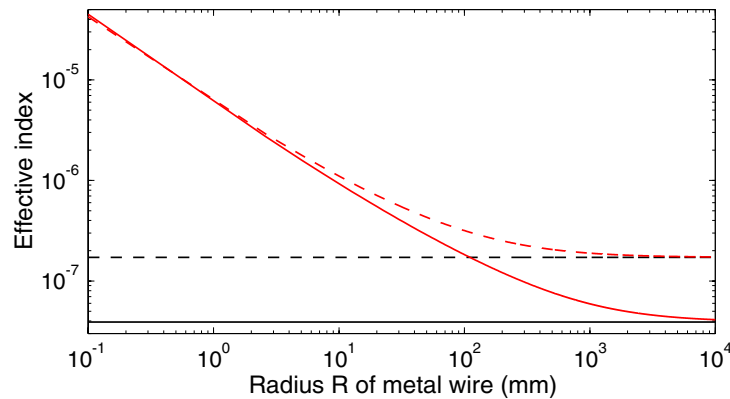


Fig. 2. Change of effective index with the radius R of metal wire. The red curves are the calculated results, and the black curves are the values given by Eq. (8). The dashed curves are $\text{Im}(n_{\text{eff}})$, and the solid curves are $\text{Re}(n_{\text{eff}}) - 1$.

To see the influence of the finite radius of the metal wire, we calculate the effective indices n_{eff} of the APSPs at the interfaces of copper wires with different R . The frequency is chosen to be 0.5 THz (i.e., $\lambda_0 = 0.6$ mm). The ϵ_m value is determined to be

$\epsilon_m = -6.3 \times 10^5 + j2.77 \times 10^6$ according to a fitted Drude formula for copper [27]. The relation $\mu_m = 1$ is used. The calculated n_{eff} values, as a function of R , are shown in Fig. 2. One can see that, just as expected, n_{eff} approach to the value determined by Eq. (8) for very large R . One can also see that, both the values of $\text{Im}(n_{\text{eff}})$ and $\text{Re}(n_{\text{eff}}) - 1$ increase with the decrease of the radius R . Thick metal wires are sometimes inconvenient for certain applications, but with lower attenuation. Therefore, one should balance between the size and the attenuation when designing a concrete metal wire waveguide.

To see the dependency on the frequency, we calculate the n_{eff} values, as a function of frequency. The metal is chosen to be copper, and the radius R is chosen to be 0.45 mm. The frequency-dependent ϵ_m of copper is obtained from the corresponding Drude formula of Ref. [27]. The calculated n_{eff} , as a function of frequency is shown in Fig. 3(a). By use of the relation $\alpha = k_0 \text{Im}(n_{\text{eff}})$, one can further obtain the attenuate coefficient α . The calculated α value is shown in Fig. 3(b). One can see that the attenuation is smaller than $2 \times 10^{-3} \text{ cm}^{-1}$ in the range of 0.1~1 THz. This result explicitly shows the superiority of a copper wire waveguide.

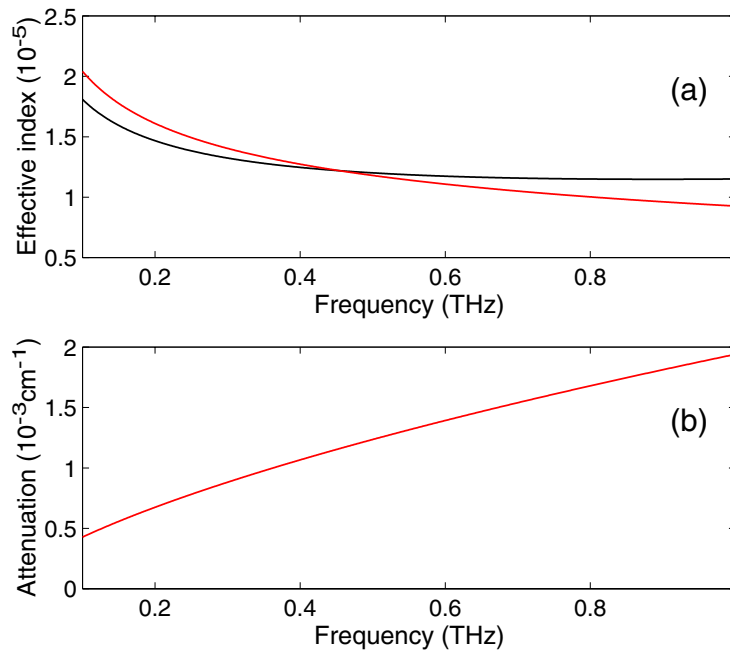


Fig. 3. (a) Change of effective index with the frequency. The red curve is $\text{Im}(n_{\text{eff}})$, and the black curve is $\text{Re}(n_{\text{eff}}) - 1$. (b) Change of attenuation with the frequency.

One may find that the attenuations shown in Fig. 3(b) here are smaller than the measured values of Ref. [17]. Also, in our calculations, the attenuation increases with increasing frequency, but an opposite trend was observed in Ref. [17]. These differences indicate that the dominant loss does not result from the attenuation of the eigenmode (i.e., APSP) itself but from other sources. We guess some other metal components that are not far away from the metal wire are probably the loss sources. As we state above, the modal field of an APSP is quite large. If some other metal components (especially magnetic metal components, note that optical tables are normally magnetic) are in the range of the modal field, then the loss will increase. In addition, through numerical calculations, we found that, for a certain metal wire, the width of the modal field increases with the decrease of the frequency. Then, the APSPs for low frequencies will have higher losses if some other metal components are not far from the metal wire, because larger modal fields have higher losses in this case.

As we state above, the beam width of an APSP is quite large, though the metal wire is thin. This property is important for the focusing application. One should be aware of the large

beam width when choosing a focusing lens. If the lens is not large enough, the truncation of the modal field may happen and lead to the loss of a lot of energy. It is worth mentioning that APSPs are related to radially polarized light beams [31-33]. Radially polarized light beams can be used for many applications, such as microscopy, optical tweezer, and optical data storage. Clearly, a metal wire waveguide also represents a viable method to generate radially polarized light beams with high purity. The drawback is the low efficiency.

4. Conclusions

We have attributed the observed THz metal wire waveguide to the propagation of an APSP, and explained the related experimental results of Ref. [17]. Some further problems, such as the choice of metal and the influence of the finite radius of metal wire, have been also discussed. In particular, we have predicted that the attenuation coefficient is smaller than $2 \times 10^{-3} \text{ cm}^{-1}$ in the whole range of 0.1~1 THz if a copper wire with a radius of 0.45 mm is used. The work presented in this paper not only provides a theoretical basis for THz metal wire waveguides, but also hopefully further paves the way for a wide range of new applications for THz sensing and imaging.